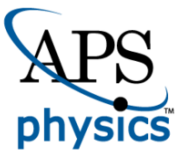



# Demonstration of a High-Fidelity span class="sc">cnot/span> Gate for Fixed-Frequency Transmons with Engineered math xmlns="http://www.w3.org/1998/Math/MathML" display="inline">mrow>mi>Z/mi>mi>Z/mi>/mrow>/math > Suppression

A. Kandala, K. X. Wei, S. Srinivasan, E. Magesan, S. Carnevale, G. A. Keefe, D. Klaus, O. Dial, and D. C. McKay

Phys. Rev. Lett. **127**, 130501 — Published 22 September 2021

DOI: 10.1103/PhysRevLett.127.130501

# Demonstration of a High-Fidelity CNOT for Fixed-Frequency Transmons with Engineered ZZ Suppression

A. Kandala,* K. X. Wei,† S. Srinivasan,‡ E. Magesan,
S. Carnevale, G. A. Keefe, D. Klaus, O. Dial, and D. C. McKay§
*IBM Quantum, IBM T.J. Watson Research Center, Yorktown Heights, NY 10598, USA*
(Dated: August 17, 2021)

Improving two-qubit gate performance and suppressing crosstalk are major, but often competing, challenges to achieving scalable quantum computation. In particular, increasing the coupling to realize faster gates has been intrinsically linked to enhanced crosstalk due to unwanted two-qubit terms in the Hamiltonian. Here, we demonstrate a novel coupling architecture for transmon qubits that circumvents the standard relationship between desired and undesired interaction rates. Using two fixed frequency coupling elements to tune the dressed level spacings, we demonstrate an intrinsic suppression of the static $ZZ$, while maintaining large effective coupling rates. Our architecture reveals no observable degradation of qubit coherence ($T_1, T_2 > 100\ \mu s$) and, over a factor of 6 improvement in the ratio of desired to undesired coupling. Using the cross-resonance interaction we demonstrate a 180 ns single-pulse CNOT gate, and measure a CNOT fidelity of 99.77(2)% from interleaved randomized benchmarking.

Quantum computing requires well-controlled, multi-qubit devices that offer speedup in certain tasks compared to their classical counterparts. Recently, there has been an explosion in device scaling, mostly based on superconducting qubits [1, 2]. However, multi-qubit circuit fidelity, and ultimately the path to a fully fault tolerant architecture, is impeded by the tradeoff between crosstalk and gate speed. This tradeoff is implicit in the canonical cQED Hamiltonian for two transmons with fixed coupling($i = \{0, 1\}$),

$$H/h = \sum_{i=\{0,1\}} \left( f_i \hat{a}_i^\dagger \hat{a}_i + \frac{\alpha_i}{2} \hat{a}_i^\dagger \hat{a}_i \left[ \hat{a}_i^\dagger \hat{a}_i - 1 \right] \right) + J(\hat{a}_0^\dagger + \hat{a}_0)(\hat{a}_1^\dagger + \hat{a}_1), \quad (1)$$

with frequencies $f_i$, anharmonicities $\alpha_i$ and coupling strength $J$ that can be engineered by a common bus resonator [3] or direct capacitance [4]. The entanglement rate is set by $J$ for a number of two-qubit gates [3, 5–8], and so, a large $J$ is desirable for fast two-qubit entangling gates. This maximizes gate fidelity given finite qubit coherence. However, in this Hamiltonian, the dressed energy levels have a two-qubit frequency shift (to second order in $J$) [9]

$$H_{ZZ} = \nu_{ZZ} |11\rangle\langle 11| \quad (2)$$

$$\nu_{ZZ} = f_{11} - f_{01} - f_{10} + f_{00}, \quad (3)$$

$$= 2J^2 \frac{\alpha_0 + \alpha_1}{(\Delta + \alpha_0)(\Delta - \alpha_1)}, \quad (4)$$

where $\Delta$ is the qubit-qubit detuning and $f_{ij}$ is the energy of the dressed state $|ij\rangle$. For fixed couplings, this is an always on source of error and referred to as the static ZZ interaction. It limits multi-qubit circuit performance [10–14], and is an impediment for realizing quantum error detection [15, 16]. The unfavorable quadratic scaling of the $ZZ$ error term puts a strict upper limit on $J$ in single coupler designs, leading to slow gates.

An alternative approach to mitigating crosstalk employs tunable coupling elements with large on/off ratios for $J$ [17–20]. The introduction of tunable elements typically leads to additional decoherence and control complexity. More recent approaches have directly focused on suppressing the static $ZZ$ interaction by engineering the two-qubit level spacings. As seen from Eqn. 4, this can be achieved by coupling qubits with opposite signs of anharmonicity [21–23]. This effect can also be achieved by employing multiple coupling paths [24–29] with tunable elements. In both approaches, the suppression of static $ZZ$ results in clear improvements to simultaneous single qubit gate performance.

In this work, we demonstrate ZZ suppression by using multiple paths made purely from fixed-frequency, non-tunable elements. The lack of tunability means the circuit is simple to control and insensitive to noise. Nonetheless, it is shown to be robust to variations in circuit parameters such as the qubit frequencies. The result is a device with an effective $J$ of 3.5 MHz, yet a $ZZ$ of only 26 kHz. We explore the physics of the cross-resonance (CR) interaction [6, 9, 10, 22, 31–34] with this novel device architecture, and demonstrate a CNOT gate with a fidelity of 99.77(2)%.

* akandala@us.ibm.com
† xkwei@ibm.com
‡ srikants@us.ibm.com
§ dcmckay@us.ibm.com

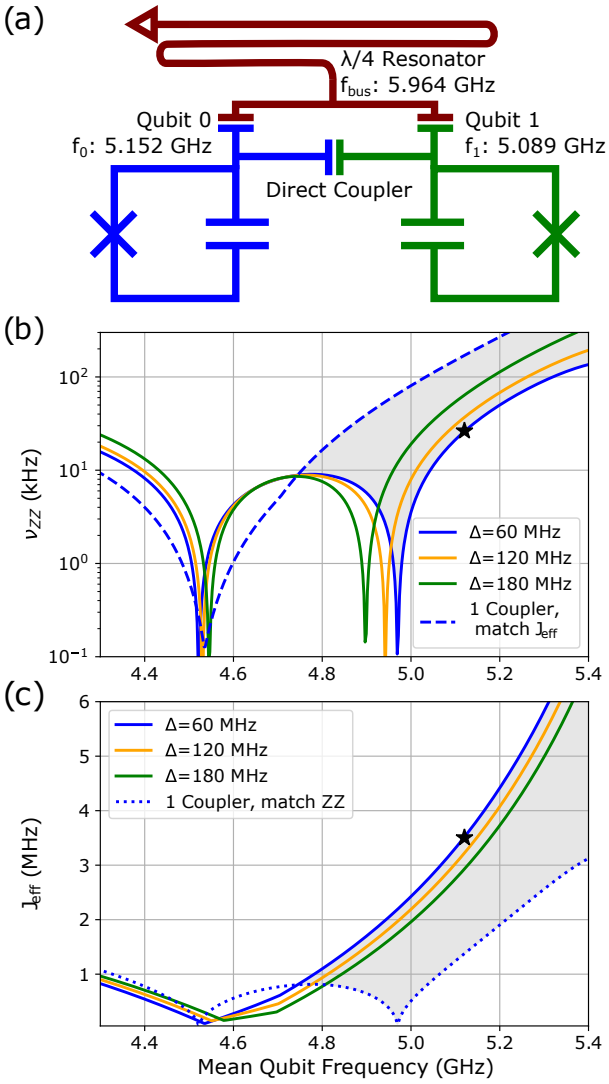


FIG. 1. (a) A circuit schematic of the multi-path coupler (MPC) device described in the main text. The device consists of two fixed-frequency transmon qubits with a direct coupler and a $\lambda/4$ resonator ($\alpha_0 = \alpha_1 = -302$ MHz, $g_0(g_1) = 88.5(87.5)$ MHz, $J_0 = 6.2$ MHz). During the course of this work, the average coherence properties for the qubits [Q0,Q1] were $T_1 = [115(11), 117(17)]$ $\mu s$ and $T_2 = [129(14), 139(32)]$ $\mu s$. (b) For these values of $g_1, g_2, J_0$ we calculate $\nu_{ZZ}$ vs the mean qubit frequency at different qubit-qubit detunings (see also Ref. [30]). The experimental data is highlighted by the star. The dashed line is the $\nu_{ZZ}$ for a pair of qubits with $\Delta = 60$ MHz coupled via a single path (for example, a direct coupler) with the same effective $J$ as the device (see part (c)). (c) The effective $J$ for the device at different qubit-qubit detunings, the experiment value is the star. The dotted line is the effective $J$ for a $\Delta = 60$ MHz direct coupler device with the same $ZZ$ rate as the device (see part (b)). The shaded region represents the frequency region where the multi-path coupler shows an improvement in $J_{\text{eff}}/\nu_{ZZ}$.

To understand this device, we start with the Hamiltonian for two transmon qubits with multiple coupling paths,

$$H/h = \sum_{i=\{0,1\}} \left( f_i \hat{a}_i^\dagger \hat{a}_i + \frac{\alpha_i}{2} \hat{a}_i^\dagger \hat{a}_i \left[ \hat{a}_i^\dagger \hat{a}_i - 1 \right] \right) + J_0 (\hat{a}_0^\dagger + \hat{a}_0)(\hat{a}_1^\dagger + \hat{a}_1) + \sum_{j=0}^{N_{\text{bus}}} f_{\text{bus},j} \hat{b}_j^\dagger \hat{b}_j + \sum_{i=\{0,1\}} \sum_{j=0}^{N_{\text{bus}}} g_{i,j} (\hat{a}_i^\dagger + \hat{a}_i)(\hat{b}_j^\dagger + \hat{b}_j), \quad (5)$$

where $J_0$ is the direct exchange coupling, and $g_{i,j}$ is the coupling from qubit $i$ to harmonic resonator mode $j$. With coupling amplitudes $g_{i,j}, J_0$ of the appropriate sign, diagonalizing the Hamiltonian of Eqn. 5 results in contributions to the energy level shifts from the multiple coupling terms and leads to an effective cancellation of the static $ZZ$ interaction. Specifically, we show that for fairly accessible coupling amplitudes, the static $ZZ$ can be suppressed over a large range of qubit frequencies in the straddling regime $|\Delta| < |\alpha_0|, |\alpha_1|$ (see § S2 of the supplement) without sacrificing the ability to enable a strong CR interaction. In this work, we realize such a multi-path coupler (MPC) device Hamiltonian by simultaneously coupling two qubits with a $\lambda/4$ CPW resonator with its fundamental mode above both qubit frequencies and a direct capacitive coupler (short CPW section); for this geometry, $g_1, g_2, J_0 > 0$. A schematic and device parameters are shown in Fig. 1(a).

We characterize the effective strength of the coupling in terms of the ability of the device to enable a CR interaction, i.e., the $ZX$ rate ($\nu_{ZX}$) generated when qubit $i$ is driven at the frequency of a neighboring qubit $j$. For small drives this rate is given as $\nu_{ZX} = \mu_{ij}\Omega$ [9] where $\Omega$ is the CR drive amplitude. For ease of comparison, we quantify this strength in terms of an effective $J$ ($J_{\text{eff,ij}}$). We numerically calculate $\mu_{ij}$ for the multi-path coupler and define

$$J_{\text{eff,ij}} = \mu_{ij} \frac{(\alpha_i + \Delta_{ij})\Delta_{ij}}{\alpha_i}, \quad (6)$$

i.e., the value of $J$ from Eqn. 1 for a single coupler that would provide the same $\mu_{ij}$. For the multipole coupler, $J_{\text{eff,ij}} \neq J_{\text{eff,ji}}$, and we define $J_{\text{eff}}$ to be for the value with the largest $\mu$. The $ZZ$ cancellation, and $J_{\text{eff}}$ are both dependent on the qubit frequencies and so we plot them as a function of mean qubit frequency and for different qubit detunings, in Fig. 1 (b) and (c), respectively. Fig. 1 (b) displays two points of sign changes of the static $ZZ$

through zero. The $\nu_{ZZ} = 0$ point at the lower mean frequency trivially corresponds to $J_{\text{eff}} \sim 0$ as seen in Fig. 1 (c). However, crucially for CR operation, the second $\nu_{ZZ} = 0$ point at higher mean frequency maintains a finite $J_{\text{eff}}$. For the $J_{\text{eff}}$ measured on the MPC device, the static $ZZ$ rate arising from an equivalent standard direct coupler is also shown for comparison in Fig. 1 (b). The difference between the dashed and solid lines demonstrates that the multi-path couplers break the typical fixed relationship between $J$ and $\nu_{ZZ}$ set by Eqn. 4. This manifests as a significant increase in the ratio of the desired coupling to the undesired coupling, $J_{\text{eff}}/\nu_{ZZ}$, over a broad range of qubit frequencies, despite the narrow bandwidth of the zero in $ZZ$ and without sacrificing the strength of $J$. Such a range of qubit frequencies is indicated by the the shaded region in Fig. 1 (b),(c). It is not necessarily optimal to operate at a $\nu_{ZZ} = 0$ point, since, for finite coherence, there is a benefit to trading off $ZZ$ for $J_{\text{eff}}$. Additionally, with fixed-frequency qubits there are limits to how close we can fabricate devices exactly at the $\nu_{ZZ} = 0$ point. For this device, $\nu_{ZZ} = 26$ kHz and $J_{\text{eff}} = 3.5$ MHz, resulting in $J_{\text{eff}}/\nu_{ZZ} \approx 130$; for an equivalent-$J$ single coupler, at the same $J$ and $\Delta$, the ratio is only $\approx 20$. In practice, there is a limit to how far the qubit frequencies should be above the $\nu_{ZZ} = 0$ point set by the desired absolute value of the $\nu_{ZZ}$, which will increase idle and simultaneous single qubit gate error. We give a plot of error vs $\nu_{ZZ}$ in Fig. S4 of the supplement; for a 200 ns gate $\nu_{ZZ} = 60$ kHz sets an error limit of 0.1%.

We now delve into the dynamic properties of the device under CR drives, which entails driving a control qubit at the frequency of the target qubit, with an amplitude $\Omega$. While the desired entangling interaction is $ZX$, the drive Hamiltonian constitutes several unwanted terms that have been studied extensively in theory and experiment [9, 10, 33]. This includes a control qubit stark shift $ZI$ rate ($\nu_{ZI}$) that is a consequence of the off-resonant tone on the control qubit. While the $ZI$ interaction is often nullified by echo-sequences, the additional single qubit gates and pulse ramps lead to a gate time cost. Instead, the approach we introduce here involves the use of calibrated frame-changes [35] on the control qubit to null the Stark shift, which has no additional time cost. However, this relies on the stability of the Stark shift, which is intrinsically related to amplitude noise of the CR pulse $\nu_{ZI} \propto \Omega^2$ [9]. In Fig. 2, we study the $ZX$ and $ZI$ interaction rates as a function of drive amplitude, measured using Hamiltonian tomography [33] and Ramsey sequences, respectively. The experimental data shows good agreement with

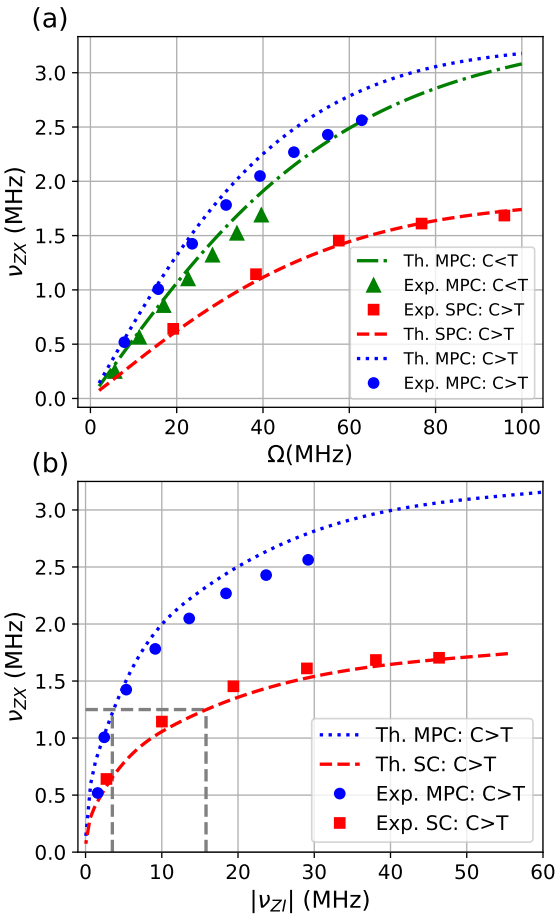


FIG. 2. (a) ZX rate ($\nu_{ZX}$ vs CR drive strength ($\Omega$) for the multi-path coupler (MPC) device and for a single-path coupler (SPC) device. Solid points represent experimental data and lines represent theory. Although the single coupling device has higher ZZ, it has a lower $ZX$ rate. For the MPC device we measure in both CR directions; when the control (C) is higher frequency than the target (T) and vice-versa. (b) The magnitude of the control stark shift ($|\nu_{ZI}|$) versus the $\nu_{ZX}$ for the two devices (the shift is negative). At the same Stark shift, the MPC device supports much larger $ZX$ rates, attributed to the greater $J_{\text{eff}}$.

numerical simulations. Note that the low drive, linear $ZX$ limit in Fig. 2(a) is employed to estimate the $J_{\text{eff}}$ discussed previously. We also compare these interaction rates to a single-path coupler (SPC) device with similar frequencies and coherence to the MPC device (see Table 1 of the supplement). The SPC device has a single direct capacitive coupler with

$J = 2.07$ MHz corresponding to a $\nu_{ZZ} = 58$ kHz ($J/\nu_{ZZ} \approx 36$); larger than the MPC device despite the lower $J$ due to the lack of a MPC's $ZZ$ cancellation. The effect of enhanced $J_{\text{eff}}$ is apparent in the comparatively larger $ZX$ rates for the MPC device, enabling faster two qubit gates. Furthermore, this also translates into a comparatively smaller $\nu_{ZI}$ on the MPC device for a desired $ZX$ rate, seen in Fig. 2(b), leading to increased stability for unechoed two-qubit gates. For example, in Fig. 2(b) we highlight that for $\nu_{ZX} = 1.25$ MHz (corresponding to a 200 ns gate without rise/fall times), the Stark shift is $\nu_{ZI} = -3.5$ MHz for the MPC device, but $\nu_{ZI} = -16$ MHz for the SPC device. If the CR amplitude drifts by 0.5% then the change in the Stark shift results in an error for the MPC device of $5 \times 10^{-4}$, but an error for the SPC device of $10^{-2}$, which is more than an order of magnitude worse.

We finally discuss the construction of a CNOT gate with our device architecture and cross-resonance. The CNOT gate is particularly useful for many algorithms, and is also advantageous for benchmarking, since it belongs to the Clifford group. Typical CNOT constructions with CR have employed echo sequences [33, 36] sandwiched between single qubit rotations. An alternate approach uses only a single CR pulse and single qubit operations, dubbed a direct CNOT, that is more efficient in total gate-time but is not naturally insensitive to low frequency amplitude noise (a similar direct CNOT was also used recently in Ref [11]). The direct CNOT gate is constructed from two physical pulses that are applied simultaneously: a CR drive on the control qubit, and a resonant drive on the target qubit. Following a rough amplitude calibration of the CR pulse for a chosen gate time, the phase of the CR drive is calibrated to minimize the $ZY$ term in Hamiltonian tomography [33], with both calibrations performed in the absence of a target drive. This is followed by a simultaneous fine calibration (using error amplification sequences [37]) of the CR/target drive amplitude, target DRAG, and CR/target drive phases such that the resultant target dynamics is a $2\pi$ rotation when the control is in $|0\rangle$ and a $X_\pi$ rotation when the control is in $|1\rangle$. The gate unitary now can be written as $U = |0\rangle\langle 0| \otimes I + e^{i\phi} |1\rangle\langle 1| \otimes X$, where $\phi$ is a phase on the control qubit generated by the CR drive, related to its Stark shift. Finally, we add a frame change [35] on the control qubit at the end of the gate to cancel $\phi$, which brings the unitary to the desired CNOT gate. As discussed previously, the suppressed Stark shift in the MPC device plays an important role in the stability of this frame change.

In Fig. 3 we show the results of our gate optimization for various gate-times. Fig. 3(a) reports an upper bound on the gate error (see caption) as a function of the gate-time. At the optimal length of 180 ns, we show interleaved randomized benchmarking [38] curves in Fig. 3(b), that we use to estimate a two qubit gate error of only $2.3\times10^{-3}$ (upper bound of $3.0\times10^{-3}$ from standard RB). Additional characterization of the gate reveals that the measured error rate is consistent with purity benchmarking, and leakage contributions to the error to be less than $10^{-4}$ (see § S5 and Fig. S3 of the supplement). It

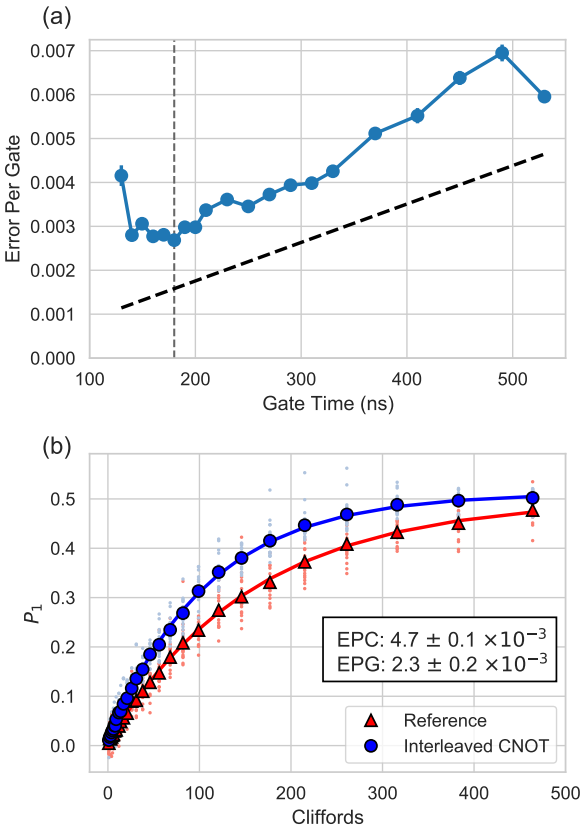


FIG. 3. (a) Finding the gate-time that optimizes the error. At each point we perform standard RB, measure the error per Clifford (EPC) and divide by the number of CNOT gates per Clifford (see § S4 of the supplement) to arrive at the error per gate (EPG). This is an upper bound on the EPG since it assumes the single qubit error contribution to the EPC is zero. The dashed line is the estimated lower bound EPG based on the measured $T_1, T_2$. (b) At the optimal gate length of 180 ns, vertical dashed line in (a), we perform interleaved RB; data shown is the probability ($P_1$) of measuring the $|1\rangle$ state for target qubit. Averaging over the measurements on the two qubits, the EPG is $2.3\times\ 10^{-3}$ (fidelity of 99.77%) and the EPC is $4.67\times10^{-3}$ which gives an error upper bound of $3.0\times10^{-3}$.

is important to highlight that the enhanced $J_{\text{eff}}$ and suppressed static $ZZ$, enable both: a state-of-the art CNOT gate constructed using cross-resonance, and the high-fidelity, simultaneous operation of 40 ns single qubit gates at an error of $3.5(1)\times10^{-4}$ and $2.7(1)\times10^{-4}$ for Q0 and Q1 respectively. This manifests in the reference RB decay of Fig. 3(b) extending to $\sim 500$ two-qubit Clifford operations.

In conclusion, we demonstrate a fixed frequency architecture for transmons with an engineered suppression of the $ZZ$ interaction term through the use of two elements – a direct capacitive coupler and a $\lambda/4$ resonator. This multi-path coupler allows the increase of effective $J$ coupling between the qubits, without the corresponding unwanted $ZZ$ interaction, i.e., breaking the standard $J/\nu_{ZZ}$ relationship of single element couplers. This enables us to realize a 180 ns single-pulse cross-resonance CNOT with an error of $2.3\times10^{-3}$, which is more than a factor of two improvement over the previous best reported error of $5\times10^{-3}$ [11] for a 273 ns gate. Since fixed-frequency superconducting processors with over 60 qubits have already been demonstrated based on cross-resonance, this work provides a clear path for superior multi-qubit circuit performance via faster two qubit gates and reduced $ZZ$ error, without any degradation of coherence or increase in control complexity.

We thank Muir Kumph, Shawn Hall and Vincent Arena for help with packaging. We acknowledge helpful discussions with Isaac Lauer, Neereja Sundaresan, Firat Solgun, Pranav Mundada, Gengyan Zhang, Thomas Hazard and Andrew Houck. The gate bring-up, investigation, and characterization work was supported by IARPA under LogiQ (contract W911NF-16-1-0114). This work includes Supplementary materials that detail the device parameters, gate tune-up and characterization, with additional references [39–41].

[1] Wei-Jia Huang, Wei-Chen Chien, Chien-Hung Cho, Che-Chun Huang, Tsung-Wei Huang, and Ching-Ray Chang, "Mermin's inequalities of multiple qubits with orthogonal measurements on ibm q 53-qubit system," Quantum Engineering , e45 (2020).

[2] Frank Arute, Kunal Arya, Ryan Babbush, Dave Bacon, Joseph C Bardin, Rami Barends, Rupak Biswas, Sergio Boixo, Fernando GSL Brandao, David A Buell, *et al.*, "Quantum supremacy using a programmable superconducting processor," Nature **574**, 505–510 (2019).

[3] L. DiCarlo, J. M. Chow, J. M. Gambetta, Lev S. Bishop, B. R. Johnson, D. I. Schuster, J. Majer, A. Blais, L. Frunzio, S. M. Girvin, and R. J. Schoelkopf, "Demonstration of two-qubit algorithms with a superconducting quantum processor," Nature **460**, 240 (2009).

[4] R. Barends, J. Kelly, A. Megrant, A. Veitia, D. Sank, E. Jeffrey, T. C. White, J. Mutus, A. G. Fowler, B. Campbell, Y. Chen, Z. Chen, B. Chiaro, A. Dunsworth, C. Neill, P. O'Malley, P. Roushan, A. Vainsencher, J. Wenner, A. N. Korotkov, A. N. Cleland, and John M. Martinis, "Superconducting quantum circuits at the surface code threshold for fault tolerance," Nature **508**, 500 (2014).

[5] S. Poletto, Jay M. Gambetta, Seth T. Merkel, John A. Smolin, Jerry M. Chow, A. D. Córcoles, George A. Keefe, Mary B. Rothwell, J. R. Rozen, D. W. Abraham, Chad Rigetti, and M. Steffen, "Entanglement of two superconducting qubits in a waveguide cavity via monochromatic two-photon excitation," Phys. Rev. Lett. **109**, 240505 (2012).

[6] GS Paraoanu, "Microwave-induced coupling of superconducting qubits," Physical Review B **74**, 140504 (2006).

[7] Jerry M Chow, Jay M Gambetta, Andrew W Cross, Seth T Merkel, Chad Rigetti, and M Steffen, "Microwave-activated conditional-phase gate for superconducting qubits," New. J. Phys. **15**, 115012 (2013).

[8] S Krinner, P Kurpiers, B Royer, P Magnard, I Tsitsilin, J-C Besse, A Remm, A Blais, and A Wallraff, "Demonstration of an all-microwave controlled-phase gate between far detuned qubits," arXiv preprint arXiv:2006.10639 (2020).

[9] Easwar Magesan and Jay M Gambetta, "Effective hamiltonian models of the cross-resonance gate," Physical Review A **101**, 052308 (2020).

[10] Neereja Sundaresan, Isaac Lauer, Emily Pritchett, Easwar Magesan, Petar Jurcevic, and Jay M. Gambetta, "Reducing unitary and spectator errors in cross resonance with optimized rotary echoes," PRX Quantum **1**, 020318 (2020).

[11] Petar Jurcevic, Ali Javadi-Abhari, Lev S Bishop, Isaac Lauer, Daniela F Bogorin, Markus Brink, Lauren Capelluto, Oktay Günlük, Toshinari Itoko, Naoki Kanazawa, Abhinav Kandala, George A Keefe, Kevin Krsulich, William Landers, Eric P Lewandowski, Douglas T McClure, Giacomo Nannicini, Adinath Narasgond, Hasan M Nayfeh, Emily Pritchett, Mary Beth Rothwell, Srikanth Srinivasan, Neereja Sundaresan, Cindy Wang, Ken X Wei, Christopher J Wood, Jeng-Bang Yau, Eric J Zhang, Oliver E Dial, Jerry M Chow, and Jay M Gambetta, "Demonstration of quantum volume 64 on a superconducting quantum computing system," Quantum Science and Technology **6**, 025020 (2021).

[12] David C. McKay, Sarah Sheldon, John A. Smolin, Jerry M. Chow, and Jay M. Gambetta, "Three-qubit randomized benchmarking," Phys. Rev. Lett. **122**, 200502 (2019).

[13] S. Krinner, S. Lazar, A. Remm, C.K. Andersen, N. Lacroix, G.J. Norris, C. Hellings, M. Gabureac,

C. Eichler, and A. Wallraff, "Benchmarking coherent errors in controlled-phase gates due to spectator qubits," Phys. Rev. Applied **14**, 024042 (2020).

[14] Ken X. Wei, Isaac Lauer, Srikanth Srinivasan, Neereja Sundaresan, Douglas T. McClure, David Toyli, David C. McKay, Jay M. Gambetta, and Sarah Sheldon, "Verifying multipartite entangled greenberger-horne-zeilinger states via multiple quantum coherences," Phys. Rev. A **101**, 032343 (2020).

[15] Maika Takita, Andrew W. Cross, A. D. Córcoles, Jerry M. Chow, and Jay M. Gambetta, "Experimental demonstration of fault-tolerant state preparation with superconducting qubits," Phys. Rev. Lett. **119**, 180501 (2017).

[16] Christian Kraglund Andersen, Ants Remm, Stefania Lazar, Sebastian Krinner, Nathan Lacroix, Graham J. Norris, Mihai Gabureac, Christopher Eichler, and Andreas Wallraff, "Repeated quantum error detection in a surface code," Nature Physics **16**, 875 (2020).

[17] S. H. W. van der Ploeg, A. Izmalkov, Alec Maassen van den Brink, U. Hübner, M. Grajcar, E. Il'ichev, H.-G. Meyer, and A. M. Zagoskin, "Controllable coupling of superconducting flux qubits," Phys. Rev. Lett. **98**, 057004 (2007).

[18] Yu Chen, C. Neill, P. Roushan, N. Leung, M. Fang, R. Barends, J. Kelly, B. Campbell, Z. Chen, B. Chiaro, A. Dunsworth, E. Jeffrey, A. Megrant, J. Y. Mutus, P. J. J. O'Malley, C. M. Quintana, D. Sank, A. Vainsencher, J. Wenner, T. C. White, Michael R. Geller, A. N. Cleland, and John M. Martinis, "Qubit architecture with high coherence and fast tunable coupling," Phys. Rev. Lett. **113**, 220502 (2014).

[19] Steven J. Weber, Gabriel O. Samach, David Hover, Simon Gustavsson, David K. Kim, Alexander Melville, Danna Rosenberg, Adam P. Sears, Fei Yan, Jonilyn L. Yoder, William D. Oliver, and Andrew J. Kerman, "Coherent coupled qubits for quantum annealing," Phys. Rev. Applied **8**, 014004 (2017).

[20] B. Foxen, C. Neill, A. Dunsworth, P. Roushan, B. Chiaro, A. Megrant, J. Kelly, Zijun Chen, K. Satzinger, R. Barends, F. Arute, K. Arya, R. Babbush, D. Bacon, J. C. Bardin, S. Boixo, D. Buell, B. Burkett, Yu Chen, R. Collins, E. Farhi, A. Fowler, C. Gidney, M. Giustina, R. Graff, M. Harrigan, T. Huang, S. V. Isakov, E. Jeffrey, Z. Jiang, D. Kafri, K. Kechedzhi, P. Klimov, A. Korotkov, F. Kostritsa, D. Landhuis, E. Lucero, J. McClean, M. McEwen, X. Mi, M. Mohseni, J. Y. Mutus, O. Naaman, M. Neeley, M. Niu, A. Petukhov, C. Quintana, N. Rubin, D. Sank, V. Smelyanskiy, A. Vainsencher, T. C. White, Z. Yao, P. Yeh, A. Zalcman, H. Neven, and J. M. Martinis (Google AI Quantum), "Demonstrating a continuous set of two-qubit gates for near-term quantum algorithms," Phys. Rev. Lett. **125**, 120504 (2020).

[21] Peng Zhao, Peng Xu, Dong Lan, Ji Chu, Xinsheng Tan, Haifeng Yu, and Yang Yu, "High-contrast ZZ interaction using superconducting qubits with opposite-sign anharmonicity," Phys. Rev. Lett. **125**, 200503 (2020).

[22] Jaseung Ku, Xuexin Xu, Markus Brink, David C. McKay, Jared B. Hertzberg, Mohammad H. Ansari, and B. L. T. Plourde, "Suppression of unwanted ZZ interactions in a hybrid two-qubit system," Phys. Rev. Lett. **125**, 200504 (2020).

[23] Xuexin Xu and M.H. Ansari, "ZZ freedom in two qubit gates," (2020), arXiv:2009.00485.

[24] Pranav Mundada, Gengyan Zhang, Thomas Hazard, and Andrew Houck, "Suppression of qubit crosstalk in a tunable coupling superconducting circuit," Physical Review Applied **12**, 054023 (2019).

[25] Fei Yan, Philip Krantz, Youngkyu Sung, Morten Kjaergaard, Daniel L Campbell, Terry P Orlando, Simon Gustavsson, and William D Oliver, "Tunable coupling scheme for implementing high-fidelity two-qubit gates," Physical Review Applied **10**, 054062 (2018).

[26] Michele C. Collodo, Johannes Herrmann, Nathan Lacroix, Christian Kraglund Andersen, Ants Remm, Stefania Lazar, Jean-Claude Besse, Theo Walter, Andreas Wallraff, and Christopher Eichler, "Implementation of conditional phase gates based on tunable ZZ interactions," Phys. Rev. Lett. **125**, 240502 (2020).

[27] Yuan Xu, Ji Chu, Jiahao Yuan, Jiawei Qiu, Yuxuan Zhou, Libo Zhang, Xinsheng Tan, Yang Yu, Song Liu, Jian Li, Fei Yan, and Dapeng Yu, "High-fidelity, high-scalability two-qubit gate scheme for superconducting qubits," Phys. Rev. Lett. **125**, 240503 (2020).

[28] Youngkyu Sung, Leon Ding, Jochen Braumüller, Antti Vepsäläinen, Bharath Kannan, Morten Kjaergaard, Ami Greene, Gabriel O. Samach, Chris McNally, David Kim, Alexander Melville, Bethany M. Niedzielski, Mollie E. Schwartz, Jonilyn L. Yoder, Terry P. Orlando, Simon Gustavsson, and William D. Oliver, "Realization of high-fidelity CZ and ZZ-free iSWAP gates with a tunable coupler," (2020), arXiv:2011.01261.

[29] J. Stehlik, D. M. Zajac, D. L. Underwood, T. Phung, J. Blair, S. Carnevale, D. Klaus, G. A. Keefe, A. Carniol, M. Kumph, Matthias Steffen, and O. E. Dial, "Tunable coupling architecture for fixed-frequency transmons," arXiv preprint arXiv:2101.07746 (2021).

[30] Peng Zhao, Dong Lan, Peng Xu, Guangming Xue, Mace Blank, Xinsheng Tan, Haifeng Yu, and Yang Yu, "Suppression of static ZZ interaction in an all-transmon quantum processor," arXiv preprint arXiv:2011.03976 (2020).

[31] Chad Rigetti and Michel Devoret, "Fully microwave-tunable universal gates in superconducting qubits with linear couplings and fixed transition frequencies," Phys. Rev. B **81**, 134507 (2010).

[32] Jerry M. Chow, A. D. Córcoles, Jay M. Gambetta, Chad Rigetti, B. R. Johnson, John A. Smolin, J. R. Rozen, George A. Keefe, Mary B. Rothwell, Mark B. Ketchen, and M. Steffen, "Simple all-microwave

entangling gate for fixed-frequency superconducting qubits," Phys. Rev. Lett. **107**, 080502 (2011).

[33] Sarah Sheldon, Easwar Magesan, Jerry M. Chow, and Jay M. Gambetta, "Procedure for systematically tuning up cross-talk in the cross-resonance gate," Phys. Rev. A **93**, 060302 (2016).

[34] Moein Malekakhlagh, Easwar Magesan, and David C. McKay, "First-principles analysis of cross-resonance gate operation," Phys. Rev. A **102**, 042605 (2020).

[35] David C. McKay, Christopher J. Wood, Sarah Sheldon, Jerry M. Chow, and Jay M. Gambetta, "Efficient $z$ gates for quantum computing," Phys. Rev. A **96**, 022330 (2017).

[36] A. D. Córcoles, Jay M. Gambetta, Jerry M. Chow, John A. Smolin, Matthew Ware, Joel Strand, B. L. T. Plourde, and M. Steffen, "Process verification of two-qubit quantum gates by randomized benchmarking," Phys. Rev. A **87**, 030301 (2013).

[37] Sarah Sheldon, Lev S. Bishop, Easwar Magesan, Stefan Filipp, Jerry M. Chow, and Jay M. Gambetta, "Characterizing errors on qubit operations via iterative randomized benchmarking," Phys. Rev. A **93**, 012301 (2016).

[38] Easwar Magesan, Jay M. Gambetta, B. R. Johnson, Colm A. Ryan, Jerry M. Chow, Seth T. Merkel, Marcus P. da Silva, George A. Keefe, Mary B. Rothwell, Thomas A. Ohki, Mark B. Ketchen, and M. Steffen, "Efficient measurement of quantum gate error by interleaved randomized benchmarking," Phys. Rev. Lett. **109**, 080505 (2012).

[39] D. I. Schuster, A. A. Houck, J. A. Schreier, A. Wallraff, J. M. Gambetta, A. Blais, L. Frunzio, J. Majer, B. Johnson, M. H. Devoret, S. M. Girvin, and R. J. Schoelkopf, "Resolving photon number states in a superconducting circuit," Nature **445**, 515 (2007).

[40] Jared B Hertzberg, Eric J Zhang, Sami Rosenblatt, Easwar Magesan, John A Smolin, Jeng-Bang Yau, Vivek P Adiga, Martin Sandberg, Markus Brink, Jerry M Chow, *et al.*, "Laser-annealing josephson junctions for yielding scaled-up superconducting quantum processors," arXiv preprint arXiv:2009.00781 (2020).

[41] David C. McKay, Stefan Filipp, Antonio Mezzacapo, Easwar Magesan, Jerry M. Chow, and Jay M. Gambetta, "Universal gate for fixed-frequency qubits via a tunable bus," Phys. Rev. Applied **6**, 064007 (2016).